



HAL
open science

Interannual dynamics of putative parasites (Syndiniales Group II) in a coastal ecosystem

Urania Christaki, Dimitra-ioli Skouroliakou, Ludwig Jardillier

► **To cite this version:**

Urania Christaki, Dimitra-ioli Skouroliakou, Ludwig Jardillier. Interannual dynamics of putative parasites (Syndiniales Group II) in a coastal ecosystem. *Environmental Microbiology*, 2023, 25 (7), pp.1314-1328. 10.1111/1462-2920.16358 . hal-04269465

HAL Id: hal-04269465

<https://hal.science/hal-04269465>

Submitted on 3 Nov 2023

HAL is a multi-disciplinary open access archive for the deposit and dissemination of scientific research documents, whether they are published or not. The documents may come from teaching and research institutions in France or abroad, or from public or private research centers.

L'archive ouverte pluridisciplinaire **HAL**, est destinée au dépôt et à la diffusion de documents scientifiques de niveau recherche, publiés ou non, émanant des établissements d'enseignement et de recherche français ou étrangers, des laboratoires publics ou privés.

1 **Interannual dynamics of putative parasites (Syndiniales Group II) in a coastal**
2 **ecosystem**

3 **Urania Christaki^{1*}, Dimitra-Ioli Skouroliakou^{1*}, Ludwig Jardillier²**

4 ¹ Univ. Littoral Côte d'Opale ULCO, Univ. Lille, UMR CNRS 8187 LOG, 62930 Wimereux,
5 France

6 ² Université Paris-Saclay, CNRS, AgroParisTech, Ecologie Systématique Evolution, 91190
7 Gif-sur-Yvette, France

8 corresponding author: urania.christaki@univ-littoral.fr

9 *the first two authors have equal contribution

10

11 Abstract

12 Temporal dynamics of Syndiniales Group II were investigated combining 18S rDNA amplicon
13 sequencing and direct microscopy counts (Fluorescence in Situ Hybridization, FISH-TSA)
14 during five years. The study was undertaken in meso-eutrophic coastal ecosystem, dominated
15 by diatoms, the haptophyte *Phaeocystis globosa* and exhibiting relatively low dinoflagellate
16 abundance (max. 18.6×10^3 cells L⁻¹). Consistent temporal patterns of Syndiniales Group II
17 were observed over consecutive years highlighting the existence of local populations.
18 According to sequencing data, Syndiniales Group II showed increasing abundance and
19 richness in summer and autumn. Dinospores counted by microscopy, were present at low
20 abundances and were punctuated by transient peaks. In summer dinospore highest abundance
21 (559×10^3 L⁻¹) and prevalence (38.5 %) coincided with the peak abundance of the
22 dinoflagellate *Prorocentrum minimum* (13×10^3 L⁻¹) while in autumn Syndiniales Group II
23 likely had more diversified hosts. Although, several peaks of dinospore and read abundances
24 coincided, there was no consistent relation between them. Ecological assembly processes at a
25 seasonal scale revealed that stochastic processes were the main drivers (80%) of the Group II
26 community assembly, though deterministic processes were noticeable (20%) in June and July.
27 This latter observation may reflect the specific Syndiniales - dinoflagellate interactions in
28 summer.

29

30 **Introduction**

31 Parasitism greatly influences ecosystem functioning by altering food web structure carbon
32 flow (Hudson *et al.*, 2006; Worden *et al.*, 2015). For example, by damaging their
33 phytoplanktonic hosts, parasites decrease the primary production that sustains the trophic web
34 (e.g., Kagami *et al.*, 2007; Rasconi *et al.*, 2011). Consequently, they produce labile dissolved
35 organic matter that can be used by heterotrophic prokaryotes and zoospores that are consumed
36 by zooplankton (Gleason *et al.*, 2008). In particular, Syndiniales which are known to infect a
37 wide range of organisms have attracted additional attention in recent decades due to their
38 repeated occurrence in sequence datasets (e.g., López-García *et al.*, 2001; Guillou *et al.*,
39 2008). High-throughput sequencing of marine planktonic communities have shown that the
40 putative parasites Syndiniales are likely to be the most abundant and diversified members of
41 the planktonic parasite community (e.g., Guillou *et al.*, 2008; Christaki *et al.*, 2017). Current
42 knowledge concerning spatio-temporal structuring and the host range of Syndiniales is
43 scarce, due to the difficulties of identifying the parasite-host consortia (e.g., Sassenhagen
44 *et al.*, 2020 and references therein). Within the order of Syndiniales, the dominance of Group
45 I is well established in coastal and open-ocean waters (e.g., Guillou *et al.*, 2008; Christaki *et*
46 *al.*, 2017; Sassenhagen *et al.*, 2020; Sehein *et al.*, 2022). [Direct observations evidenced](#)
47 [association of members of Group I with ciliates \(review by Skovgaard *et al.*, 2014\)](#) and single
48 cell amplification has suggested that Group I could be associated to diatoms (Sassenhagen *et*
49 *al.*, 2020). Syndiniales Group II association with dinoflagellates has been directly evidenced
50 through microscopic observations of hybridized cells (e.g., Chambouvet *et al.*, 2008; Salomon
51 *et al.*, 2009; Siano *et al.*, 2011) thanks to specific FISH probes (Chambouvet *et al.*, 2008) and
52 has been also indirectly inferred via statistical approaches using metabarcoding data (e.g.
53 network analysis, Christaki *et al.*, 2017; Anderson and Harvey, 2020). [The life-cycle of these](#)
54 [parasites is well understood since 1964 \(Chacon, 1964\). It is characterized by an alternation](#)

55 between a biflagellated free-living infective stage (the dinospore) and an intracellular stage
56 (the trophont) which grows and can expand up to filling the whole host cell. The maturation
57 of the trophont lasts a few days and can eventually kill the host and release a motile worm-
58 shaped multinucleated and multiflagellated structure (the vermiforme). It can then release
59 within a few hours hundreds of dinospores, each potentially capable of infecting a novel host
60 (Cachon 1964, Coats and Park, 2002).

61 Owing to the potential of Syndiniales Group II to **terminate** toxic dinoflagellate blooms most
62 of the previous studies focusing on these algae's have been restricted to environments and
63 periods in relation to dinoflagellate blooms (Chambouvet *et al.*, 2008; Alves-de-Souza *et al.*,
64 2012; Velo-Suárez *et al.*, 2013). High prevalence of Syndiniales is usually associated with
65 marked densities of host organisms, stratification, and may be influenced by the availability in
66 nutrients (Alves-de-Souza *et al.*, 2015; Sehein *et al.*, 2022) though it has also been reported
67 that dinospores (free-living, small flagellated Syndiniales forms, typically <10 µm) were able
68 to infect dinoflagellates at relatively low dinoflagellate abundances (Salomon *et al.*, 2009) and
69 in oligotrophic waters (Siano *et al.*, 2011).

70

71 The main objective of this study was to investigate the temporal dynamics of Syndiniales
72 Group II in a productive constantly mixed coastal system - the Eastern English Channel
73 (EEC). The EEC is characterized by diatom communities punctuated by spring blooms of the
74 haptophyte *Phaeocystis globosa* and exhibiting relatively low dinoflagellate abundances (e.g.,
75 Grattepanche *et al.*, 2011). A previous temporal survey in the same area revealed the
76 occurrence of Syndiniales and provided insights into their temporal dynamics inferring their
77 potential hosts through network analysis (Christaki *et al.*, 2017). However, co-occurrence
78 networks allow inferring putative associations **but do not necessarily reveal real interactions**.
79 Direct observations are needed to identify microbial interactions such as parasitism.

80 Parasitic taxa usually present short transient peaks, i.e. their abundance is usually low or
81 below detection limit and they occasionally increase to a noticeable abundance at the
82 community level. They can feature annual and inter-annual distributions identified as
83 'Conditionally Rare Taxa' (CRT, Shade *et al.*, 2014). The frequency of a conditionally rare
84 taxa's abundance over time exhibits a bimodal distribution (Shade *et al.*, 2014). Furthermore,
85 because the overall community assembly processes is critical in tracking and predicting future
86 changes in planktonic communities (e.g Ramond *et al.*, 2021; Skouroliakou *et al.*, 2022; Xu
87 *et al.*, 2022, and references therein), an exploratory analysis was undertaken for Syndiniales
88 Group II at a seasonal scale applying the null model analysis framework (Stegen *et al.*, 2012,
89 2013). Community assembly describes how processes interact to determine species
90 composition and local biodiversity of a community (e.g., Chase and Myers, 2011). The
91 *rationale* here was that while ecological deterministic processes are conducive to modeling,
92 stochastic ones are far less predictable. The main question in this study is whether stochastic
93 and deterministic ecological processes varied across seasons for Syndiniales Group II. Our
94 hypothesis was that stochastic ecological processes occur a larger scale in the microbial
95 communities and may therefore prevail in Syndiniales Group II community assembly (e.g.
96 Skouroliakou *et al.*, 2022) .

97 Overall, this study focused on the following specific questions: (i) On a technical aspect, is
98 sequencing an accurate method to infer dinospore abundances? (ii) Do Syndiniales Group II,
99 have seasonal patterns and do they relate to dinoflagellate dynamics? (iii) Stochastic or
100 deterministic ecological assembly processes prevail in the Syndiniales Group II community
101 assembly?

102 To answer these questions, a multiple year temporal survey at two different frequencies was
103 conducted to better capture the temporal changes of planktonic communities (bi-weekly
104 during 2016-2020 and at a higher frequency during 2018-2020). 18S rDNA amplicon

105 Illumina Mi-Seq sequencing and dinospore enumeration were combined with the FISH-TSA
106 method, microscopical examination of microplankton, and flow cytometry for nano- and
107 picoplankton, along with [measurements of](#) environmental parameters.

108

109 **Experimental Procedures**

110 *Study site, sample collection*

111 Samples were collected at 2 m depth at five neighboring stations between March 2016 and
112 October 2020 (Fig. S1) using 12 L Niskin bottles. From 2016 to 2020, the SOMLIT coastal
113 S1 and the offshore S2 stations (French Network of Coastal Observatories;
114 <https://www.somlit.fr/>) were sampled bi-weekly (Table 1). Stations (R1, R2, and R4)
115 belonging to the 'DYPHYRAD' transect situated about 15km north of the SOMLIT
116 stations (Fig. S1, Table 1) were sampled weekly. Higher frequency samplings (2-3 times a
117 week) were also carried out after the end of the spring bloom in June-July and in autumn in
118 September-October at stations R1 and R4. [The higher frequency was applied in an effort to](#)
119 [catch rapidly changing dinoflagellate and Syndiniales Group II abundance dynamics.](#)
120 [Phaeocystis globosa](#) spring bloom occurs every year in April-May (e.g Breton, *et al.*, 2011,
121 2017; 2021 Grattepanche, *et al.* 2011; Christaki *et al.*, 2014, 2017; Breton *et al.*, 2021). The
122 [post spring bloom and autumn periods were chosen because higher Syndiniales Group II and](#)
123 [/or dinoflagellate abundances were observed during these periods in previous studies \(eg.](#)
124 [Grattepanche, et al., 2011; Christaki et al., 2017\).](#) Only three samples were collected in
125 August due to the unavailability of the boat crew during their annual leave. For this reason,
126 the August data are presented but not further discussed.

127

128 *Environmental variables*

129 Seawater temperature (°C) and salinity were measured *in situ* using a conductivity-

130 temperature-depth profiling system (CTD Seabird SBE 25). The average subsurface daily
131 PAR experienced by phytoplankton in the water column for a six-day period before sampling
132 was obtained using a global solar radiation (GSR, Wh m⁻²) recorded by the Copernicus
133 Atmosphere Monitoring Service (CAMS) radiation service ([http://www.soda-pro.com/web-](http://www.soda-pro.com/web-services/radiation/cams-radiation-service)
134 [services/radiation/cams-radiation-service](http://www.soda-pro.com/web-services/radiation/cams-radiation-service)). GSR was converted into PAR by assuming PAR to
135 be 50% of GSR and by considering $1 \text{ W m}^{-2} = 0.36 \text{ E m}^{-2} \text{ d}^{-1}$ (Morel and Smith, 1974).
136 Inorganic nutrient concentrations (nitrate, NO₃⁻), nitrite (NO₂⁻), phosphate (PO₄³⁻), and
137 silicate (Si(OH)₄) were analysed according to Aminot and K  rouel (2004). Chlorophyll *a*
138 (Chl-*a*) concentrations were measured by fluorometry (Lorenzen, 1966). Wind speed (m s⁻¹),
139 wind direction (deg), and rainfall (kg m⁻²) were obtained from the National Aeronautics and
140 Space Administration (NASA) and Goddard Space Flight Center
141 (<http://gmao.gsfc.nasa.gov/reanalysis/MERRA-2>, resolution 0.625°×0.5°, longitude x
142 latitude). Wind stress (Pa) was calculated from wind speed as described in Smith, (1988).
143 Additional details on environmental data acquisition and sample analysis can be found at
144 <https://www.somlit.fr/>.

145

146 *DNA barcoding, bioinformatic analysis*

147 Four to seven liters of seawater [depending on the quantity of particulate matter in the water,](#)
148 [i.e until clogging of the filter](#)) were filtered onto 0.2µm polyestersulfone (PES)
149 membranes (142mm, Millipore, U.S.A.) after a pre-screening step through 150 µm nylon
150 mesh (Millipore, U.S.A.) to remove metazoans. Filters were stored at -80°C for 18S rDNA
151 amplicon Illumina MiSeq sequencing. DNA extraction was performed according to the
152 DNAeasy PowerSoil kit protocol (QIAGEN, Germany). To describe protist diversity, the V4
153 hypervariable region of the 18S rDNA gene (527 bp) was amplified using the primers EK-
154 565F (5'-GCAGTTAAAAAGCTCGTAGT) and UNonMet (5'-

155 TTTAAGTTTCAGCCTTGCG) biased against Metazoa (Bower *et al.*, 2004). Pooled and
156 purified amplicons were then paired-end sequenced on an Illumina MiSeq 2 × 300
157 platform by Genewiz (South Plainfield, NJ, USA).

158 Quality filtering of reads, identification of amplicon sequencing variants (ASV), and
159 taxonomic affiliation based on the PR2 database (Guillou *et al.*, 2013) were done in the R-
160 package DADA2 (Callahan *et al.*, 2016). A total number of 41,179 ASVs were identified
161 from 6,366,087 reads in 287 samples containing Metazoa, Streptophyta, Excavata,
162 Alveolata, Amoebozoa, Apusozoa, Archaeplastida, Hacrobia, Opisthokonta, Rhizaria,
163 and Stramenopiles. ASVs affiliated to Excavata, Metazoa, Streptophyta,
164 unaffiliated ASVs and singletons were removed, obtaining a phyloseq object
165 containing 20,651 taxa by eight taxonomic ranks. After eliminating samples with less than
166 5,000 reads, the number of reads per sample was rarefied to the lowest number of reads
167 (5,234) which produced 15,250 ASVs distributed in 269 samples. Then, only taxa affiliated
168 to the order Syndiniales Group II were kept, resulting in a new phyloseq object composed of
169 663 taxa detected in 269 samples (for more details on DNA barcoding and bioinformatic
170 analysis, see Suppl. Information). Raw sequencing data have been submitted to the Short
171 Read Archive under BioProject number PRJNA851611.

172

173 *Fluorescent in situ Hybridisation (FISH-TSA)*

174 Fluorescent in situ hybridization (FISH) coupled with tyramide signal amplification (TSA)
175 was used to enumerate Syndiniales Group II dinospores and observe infected hosts.
176 [Dinospores and infected hosts were enumerated on the same hybridized filters.](#) Samples (300
177 mL) were fixed with paraformaldehyde (1% final concentration) for 1 hour at 4°C and then
178 filtered onto 0.6 µm polycarbonate membranes. The filters were dehydrated by several
179 successive ethanol baths (50%, 70%, and 100%) and stored at -80°C until analysis. The

180 oligonucleotide probe ALV01 (5'-GCC TGC CGT GAA CAC TCT-3') was used to target
181 Syndiniales Group II dinospores (Chambouvet *et al.*, 2008). A total of 199 filters over the
182 period 2018-2020 were proceeded with FISH-TSA following the protocol described in
183 (Piwosz *et al.*, 2021 and references therein). Following the TSA reaction, the filters were
184 counter stained 15 min with calcofluor (100 ng ml⁻¹) to visualise armored
185 dinoflagellates. All counts were performed with an epifluorescence microscope at 100x
186 (Zeiss Imager M2) with different fluorescence filters (for calcofluor, excitation: 345 nm;
187 emission: 475 nm), promidium iodide (excitation: 536 nm; emission: 617 nm) and FITC
188 (excitation: 495 nm; emission: 520 nm). For dinospore counts, 150 optical fields at x100
189 corresponding to 873±149 µl of initial sample (390-1333 µl) were observed for each filter (for
190 more details see Suppl. Information).

191

192 *Microscopic and cytometric counts (morphological data)*

193 For diatoms and *P. globosa* colonies and free cells counting, 110 mL water samples
194 were collected and fixed with Lugol's-glutaraldehyde solution (1% v/v, which does not
195 disrupt *P. globosa*'s colonies, Breton *et al.*, 2006). For dinoflagellates, another 250 mL were
196 fixed with acid Lugol's solution (1% v/v) (data for dinoflagellates are available for 2018-
197 2020, Table 1). Microplankton was identified to the genus or species level when possible
198 using an inverted microscope (Nikon Eclipse TE2000-S) at 400x magnification after
199 sedimentation in a 10, 50, or 100 mL Hydrobios chamber, as described previously in (Breton
200 *et al.*, 2021). The abundance of pico- and nanophytoplankton (PicoNano, 0.2-20 µm) were
201 enumerated by flow cytometry with a CytoFlex cytometer (Beckman Coulter). For all
202 samples, 4.5 ml were fixed with paraformaldehyde (PFA) at a final concentration of 1% and
203 stored at -80 °C until analysis (Marie *et al.*, 1999). Phytoplankton cells were detected
204 according to the autofluorescence of their pigments (Chl-a). Heterotrophic nanoflagellates

205 (HNF) were enumerated after staining with SYBRGreen I following (Christaki *et al.*, 2011).

206

207 *Abundance distribution and community assembly of Syndiniales Group II*

208 Shade *et al.*, (2014) suggested a simple method for detecting conditionally rare taxa (CRT)
209 based on the coefficient of bimodality (b) defined by Ellison (1987),

$$210 \quad b = (1 + \text{skewness}^2) / (\text{kurtosis} + 3) \quad (1)$$

211 According to Shade *et al.*, (2014) when $b > 0.9$, taxa are conditionally rare (CRT). The “b”
212 coefficient was calculated for abundant ASVs representing a relative abundance ≥ 0.01 in the
213 Syndiniales Group II (this corresponded ≥ 500 reads, and 72 % of the total Syndiniales Group
214 II reads). For comparison, the bimodality coefficient was also calculated for the 55 ASV with \geq
215 100 reads (84% of the total reads).

216 To explore the ecological assembly processes regulating Syndiniales Group II at a seasonal
217 scale null models based on metabarcoding data were applied according to Stegen’s framework
218 (Stegen *et al.*, 2012, 2013) reviewed by Zhou and Ning (2017). Briefly, the community
219 assembly analysis is based on the comparison of observed community turnovers (shifts in
220 composition across samples), phylogenetic turnovers (shifts in composition weighted by the
221 phylogenetic similarity between taxa), and turnovers expected by chance (in null-models).
222 This information is used to estimate whether the differences between pairs of communities are
223 explained by dispersal, selection, or ecological drift. According to this framework,
224 deterministic processes are divided into homogeneous selection (i.e., consistent abiotic or
225 biotic conditions filter which parasites can persist) and heterogeneous selection (i.e., high
226 compositional turnover caused by shifts in environmental factors or hosts). Stochastic
227 processes are divided into homogeneous dispersal (i.e., low compositional turnover caused by
228 high dispersal rates), dispersal limitation (i.e., high compositional turnover caused by a low
229 rate of dispersal), and ecological drift that can result from fluctuations in population sizes due

230 to chance events (Table 2). The implicit hypothesis is that phylogenetic conservatism exists,
231 which means that ecological similarity between taxa is related to their phylogenetic similarity
232 (i.e., phylogenetic signal) (Losos, 2008). The Mantel correlogram was applied to detect
233 phylogenetic signal (e.g., Liu *et al.*, 2017; Doherty *et al.*, 2020, for details see Suppl.
234 Information). The phylogenetic temporal turnover (betaNRI) between pairwise communities
235 among sampling dates was quantified to investigate the action of deterministic and stochastic
236 ecological processes with *microeco* R-package v.0.6.0 (Liu *et al.*, 2021), using the
237 *trans_nullmodel* function. The phylogenetic distance between pairwise communities (beta
238 mean pairwise distance: β MPD) was computed with null models based on 999
239 randomizations with the random shuffling of the phylogenetic tree labels, as in Stegen *et al.*,
240 (Stegen *et al.*, 2013). All definitions of the different assembly processes corresponding to the
241 values of β NRI are shown in Table 2. Non-weighted metrics were used as metabarcoding data
242 are semi-quantitative and the rarefied dataset was considered to prevent any bias due to
243 potential under-sampling (Ramond *et al.*, 2021). [All analyses were ran with R version 4.1.0](#)
244 [\(R core team 2021\)](#). For more details see Suppl. Information.

245

246 **Results**

247 *Environmental variables*

248 The environmental variables showed seasonal patterns typical of temperate marine waters.
249 Nutrient inputs originated mainly from local rivers and reached relatively high values during
250 autumn and winter with the highest values in February (Fig. S2A). The N/P ratio was highly
251 variable ranging from 0.4 to 316, strongly deviating most of the time from the Redfield ratio
252 (N/P=16, Redfield, 1958). Overall, the environmental variables were of the same range and
253 showed the same seasonal variations at all stations. A comparison of the mean ranks (Kruskal
254 Wallis and Nemenyi post hoc test) of environmental variables between the different stations

255 revealed significant differences in salinity, phosphate, silicate, and Chl-*a* between the stations
256 (Fig. S2B). Principal Component Analysis (PCA) performed on the environmental dataset
257 showed a seasonal pattern opposing winter and summer conditions. Overall, summer and
258 autumn samples formed tighter groups on the PCA biplot than spring and winter samples
259 which were more dispersed (Fig. S3).

260

261 *Planktonic eukaryotic diversity and abundance*

262

263 Microscopic counts of diatoms and *Phaeocystis globosa*, and flow-cytometric counts of pico-
264 nanophytoplankton showed that diatoms were always abundant with highest abundances from
265 winter to early summer (range 4×10^3 - 5×10^6 cells L⁻¹, Fig. 1A). *P. globosa* bloomed in
266 April and May, reaching a peak of 3.6×10^7 cells L⁻¹ (Fig. 1B). Pico-nanophytoplankton
267 showed clear seasonal variations, with the highest abundance in early summer after the
268 phytoplankton spring bloom and then in autumn (Fig. 1C). Heterotrophic nanoflagellates
269 highest values were recorded each year in May - June after the spring phytoplankton bloom
270 (range 0.2×10^6 - 1.8×10^7 cells L⁻¹, Fig. 1D). Dinoflagellates -although they presented the
271 highest number of reads- were three orders of magnitude less abundant than diatoms (ranging
272 from 0.76 to 18.6×10^3 cells L⁻¹). Dinoflagellates reached their lowest abundances in winter
273 and highest in summer after the end of *P. globosa* bloom (Fig. 1E). *Gymnodinium spp.* was
274 the most abundant dinoflagellate genus in almost all samples while two other dinoflagellates
275 (*Prorocentrum minimum* and *Scrippsiella spp.*) showed moderate increases in summer (Fig.
276 S4). Ciliates presented relatively low abundances from <100 cells L⁻¹ to 7.4×10^3 cells L⁻¹
277 (Fig. 1F).

278 [Sequence data showed that](#) the most abundant group in terms of number of reads was
279 Dinophyceae (30%), followed by Bacillariophyta (25%), and Syndiniales (10%) (Fig. 2A).

280 Within Syndiniales, Group I was the most abundant (61 %, 6 Clades, 285 ASVs, Fig. 2B)
281 while Group II was the most diversified (35 %, 27 Clades, 663 ASVs). Within Syndiniales
282 Group II, Clades 10, 11, and 8 dominated (21, 25 and 9 % of the reads, respectively, Fig. 2C).
283 Syndiniales Group II showed highest abundance and richness in June, July, and September
284 and lowest in winter; the highest number of reads occurring in June 2018 (Fig. 3 A, B).
285 Fifteen samples showed high Syndiniales Group II abundance (> 600 reads, Fig. 3A). Clade 8
286 was the most abundant clade in terms of reads, followed by Clades 10, 11, 14, 30, 5, and 13,
287 respectively (Fig. S5). The most important peaks were observed at the beginning of summer
288 and autumn (Fig. 3A-B). While the summer peaks were mostly dominated by Clade 8, a
289 variety of clades and ASV dominated in the autumn peaks (Fig. S5). The highest values of
290 Syndiniales Group II read abundance and richness were recorded at station R1 which was the
291 closest to the coast but also the most visited (Fig. S6 A-B, Table 1). The cumulative number
292 over time of ASVs affiliated to Syndiniales Group II **constantly increased**. The cumulative
293 plot based on new ASVs between two consecutive dates revealed **that the slope of the**
294 **cumulative curve became steeper with the influx of new ASVs in summer and autumn** as well
295 as in autumn 2020 due to a particular high number of new ASV (Fig. S7).
296
297 Dinospores **cells were counted by microscopy (on FISH-TSA hybridized filters)** ranged from
298 undetectable to $5.6 \times 10^5 \text{ L}^{-1}$ (Fig. 3C) and generally followed a seasonal pattern similar to the
299 one of dinoflagellate **microscopy** abundances (Figs. 1E, 3C). The highest values of dinospore
300 abundance were also recorded at station R1 (Fig. S6C Table 1). **Although dinospore**
301 **abundances followed similar seasonal patterns with Syndiniales Group II reads** (Fig. 3A-C,
302 2E), **the number of reads cannot be used as a predictor of the number of dinospores and vice**
303 **versa as there was no consistent numerical relationship between them** (Fig. S8).
304

305 *Syndiniales Group II occurrence and potential hosts*

306 The maximum likelihood tree of the 20 most abundant *Syndiniales* Group II ASVs (i.e. ASVs
307 representing at least 1% of the reads affiliated to *Syndiniales* within the rarefied dataset),
308 showed that ASVs belonging to Clade 8 (ASV13 and ASV124) were the most phylogenetically
309 distant from the rest of the Clades present. Clades 10, 11, and 14 were those phylogenetically
310 closer to each other (Fig. 4). The majority of the most abundant ASVs were present every year
311 at low or very low abundances and showed a few transient peaks. Indeed, 13 out of the 20
312 ASVs were found every year, while 7 were absent at least one year and up to three years (Fig.
313 4). Among these most abundant ASVs, several ones can be characterized as "highly persistent"
314 such as ASV13 (Clade 8), ASV50 (Clade 4) and ASV101 (Clade 4), since they were present
315 every year and in more than 50% of all samples (Fig. 4). At the opposite, ASV401 (Clade 6),
316 ASV439 (Clade 47) were found only in 2019 and 2020 (5% of the samples) where they showed
317 a unique peak.

318 Prevalence of infection was assessed when hosts were abundant enough to make accurate
319 microscopy observations. Hosts were clearly identified **only** during two infection events
320 (Table 2). The first observed infection occurred during the *P. minimum* increase (up to $1.3 \times$
321 10^3 L^{-1}) **coinciding** with the dominance of Clade 8 (ASV 13) and the second was related to *P.*
322 *micans* and *Scrippsiella spp.* and **coinciding** again to the dominance of Clade 8 in July 2019
323 (Table 2). Infected cells were rare and/or not possible to identify based on their morphology
324 in the other samples although dinospores were detected. Host morphologies were diverse and
325 represented athecate and thecate dinoflagellate cells and a few cells resembling **to** ciliates.
326 Trophont and veriform like *Syndiniales* were rarely observed in the samples (Fig. S9). It is
327 worth noting, that microscopy observations of *P. globosa* and diatom cells, which reached
328 very high abundances during the study, showed no sign of infection by *Syndiniales* Group II.
329

330 *Abundance distributions and Syndiniales Group II Community Assembly*

331 For the 20 most abundant ASVs (≥ 0.01 relative abundance), the coefficient of bimodality
332 varied from 0.62 to 0.99 with only **three** ASVs identified as conditionally rare taxa ($b > 0.9$
333 ASV401 and ASV439). Applying the same calculation to the ASVs having ≥ 100 reads, the
334 result was similar as the factor “b” varied between 0.62 and 0.99 and only **five** additional ASVs
335 were detected as conditionally rare ($b > 0.9$, see also Fig. S10).

336 The potential of stochasticity vs determinism regulating the Syndiniales Group II community
337 was explored, and then, the associated ecological processes were quantified.

338 The Mantel correlograms indicated phylogenetic signals at short phylogenetic distances (10-
339 30 %, Fig. S11). The phylogenetic temporal turnover (β NRI) values ranged from -2 to 4.6
340 (Fig. 5A). The monthly variability of β NRI showed that the median value was between -2 and
341 2, defining stochastic assembly processes in Syndiniales Group II. However, β NRI values
342 were somewhat greater than 2 defining 'determinism' in June and July (Fig. 5A Table 2). The
343 null model analysis suggested that 'ecological drift' was the major ecological process
344 regulating the community assembly of Syndiniales Group II (80 %) with heterogenous
345 selection accounting for 20% (Fig. 5B).

346

347 **Discussion**

348

349 In the present study, microscopy and flow cytometry were used to quantify pico- and nano-
350 microplankton as well as dinospores, while metabarcoding data provided an extended
351 evaluation of their diversity. The present study is original in its observation frequency -less
352 than a week - and the duration of the survey - over a multiple of years -. In addition, contrary
353 to most previous studies, it was conducted in a meso-eutrophic coastal area with an expected
354 low-host abundance of dinoflagellates and Syndiniales Group II.

355

356 *Environmental context*

357 During this study, environmental variables showed clear seasonal patterns typical of the
358 Eastern English Channel (EEC; e.g., Grattepanche *et al.*, 2011; Breton *et al.*, 2017, Fig.
359 S2A). This coastal area is highly dynamic, characterized by a mega-tidal hydrological regime
360 and strong tidal currents parallel to the coast, with coastal water drifts towards the
361 shoreline. Thus, the less salty and more turbid near-shore waters remain separated from the
362 open sea by this tidal front (Brylinski *et al.*, 1991; Lagadeuc *et al.*, 1997; Senchev *et al.*,
363 2006). The stations nearer to the coast (R1, S1) - being more influenced by coastal run-off -
364 showed several extreme values of environmental variables (Genitsaris *et al.*, 2016, Fig. S2B)
365 and also the highest chlorophyll-a concentrations (Fig. S2B) and dinospore abundance (R1,
366 Fig. 3C). Since dinoflagellates proliferate in relatively warm, stratified and nutrient enriched
367 waters (Smayda, 2002), the highly dynamic hydrological conditions and the absence of
368 stratification can explain the relatively low dinoflagellate abundances in this area. In the EEC,
369 while dinoflagellates showed their highest abundances during the summer months
370 (Grattepanche *et al.*, 2011), these abundances remain relatively low compared to diatoms and
371 nano- picoplankton (Fig. 2) and to other close or distant coastal areas (Table 4).

372

373 *Sequence vs. abundance data, is sequencing an accurate method to infer dinospore*
374 *abundances?*

375 The comparison of the abundances of taxa obtained by sequencing (relative abundance of
376 reads) and microscopy (cell abundance) is not straightforward. *In silico* analysis considering
377 zero mismatches revealed that the ALV01 probe sequence matched with 80% of the ASVs
378 (corresponding to 83.5 % of the total reads) affiliated to Syndiniales Group II found in this
379 study. These results suggest that a relative increase in Syndiniales Group II reads was

380 generally the consequence of an increase in dinospore abundance measured by FISH-TSA
381 counts. This was the case in summer, in general, and autumn 2018 and 2019, in particular.
382 Conversely, there was no [relation between the dinospore abundance counted by microscopy](#)
383 and the read abundances (Fig. S8). This result implies that the dinospore abundance cannot be
384 used as a predictor of relative read abundance and *vice-versa*. This discrepancy can be
385 explained by: (i) Metabarcoding captures all cells while FISH-TSA targets only active cells.
386 Massana *et al.*, 2015 reported that Group I and Syndiniales Group II were found about 4-
387 times more in RNA relative to DNA data; (ii) there is a lag time of about 2-3 days between
388 the infection and the spore release (e.g., Coats and Park, 2002; Alves-de-Souza *et al.*, 2015);
389 (iii) it cannot be ruled out that several abundant Group II taxa were missed, although the
390 estimated *in silico* coverage of the probe was high.

391

392 *Syndiniales Group II communities and temporal patterns.*

393 In this study, Group II was, as expected, the most diversified Syndiniales group (Guillou *et al.*,
394 2008), accounting for 27 out of the 44 identified clades. Syndiniales Group II reads were
395 always recorded and, in a few cases, very abundant. The sampling effort during this study was
396 intensified during the last two years of the survey (2018-2020), with an increase in the
397 frequency of 25-30 samples/year to 70-75 samples/year, producing a total of 269 samples. The
398 cumulative plots of ASV affiliated to Syndiniales Group II did not reach a plateau and new
399 ASV between two consecutive dates (defined as 'new arrivals' herein) were detected until the
400 end of the study (Fig. S8 A, B). These intriguing observations may be explained by the
401 introduction of new taxa via transportation of water masses travelling northwards in the English
402 Channel. However, our data also showed consistent temporal patterns providing an indication
403 of the existence of 'local populations'. The repeating patterns of the most abundant clades and
404 ASVs have already been observed in two previous studies (Chambouvet *et al.*, 2008; Christaki

405 *et al.*, 2017). Indeed, dominant taxa of Syndiniales Group II varied from one year to the other,
406 though most of them were detected every year (Fig. 4). The bimodality coefficient (*b*) showed
407 that only three among the 20 most abundant ASVs (≥ 0.01 relative abundance) were identified
408 as 'Conditionally Rare Taxa' ($b > 0.9$) i.e., their abundance was usually low or below detection
409 limit and they occasionally increased to an abundance 'appreciable' at the community level
410 (*sensu* Shade *et al.*, 2014, see also M+M). The majority of ASVs exhibited a “*b*” coefficient
411 lower than 0.9, suggesting that they had seasonal and/or irregular dynamics (Shade *et al.*,
412 2014).

413 In a previous two and a half years survey in the same area, Syndiniales Group II was
414 dominated by Clades 30, 8, and 10+11 (16, 13 and 7% of total Group II reads, Christaki *et al.*,
415 2017), in the present study Clades 8, 10-11, and 14 dominated (Fig. 1C). Among these clades,
416 only Clade 14 was known to reach high abundances related to dinoflagellate blooms in summer
417 in the North-Western English Channel (Chambouvet *et al.*, 2008). Clade 8 has not been
418 reported previously as dominant in the [North-Western](#) English Channel (Chambouvet *et al.*,
419 2008) or in other long term coastal studies (e.g., Käse *et al.*, 2021, [their](#) suppl. material). This
420 clade was clearly dominating within the Group II community (25.5 % of the reads), prevailing
421 in 8 out of the 15 samples that showed important peaks (>600 reads). Clade 8 also showed the
422 highest [occurrence](#) during all years, being present in up to 97 % of the samples (in 2018, Fig.
423 4).

424 Dinospores were present throughout the sampling period at low abundances (ca. 10^3 cells L^{-1})
425 and were punctuated by a few transient peaks (ca. 10^5 cells L^{-1}). In a modeling study, the
426 critical carrying capacity that ensures stable coexistence of dinoflagellate host and parasitoid
427 varied from 10^3 to $10^5 L^{-1}$ (Salomon and Stolte, 2010). The dinospore abundances observed
428 here imply that there is a 'seed population' that could rapidly develop when the hosts reach a
429 certain abundance. However, grazing by heterotrophic dinoflagellates and ciliates of the

430 dinospores is most likely another important factor that keeps dinospore populations under
431 control since their size fits within the range of their prey's size range (e.g. Sherr and Sherr,
432 2002; Grattepanche *et al.*, 2011)

433

434 *Dinospore and Dinoflagellates dynamics*

435 In natural systems, the strength of infection by Syndiniales Group II has been related to
436 the abundance of the dinoflagellate hosts because higher hosts density enhances encounter
437 rates (Park *et al.*, 2004). Consequently, dinoflagellate blooms are associated with the increase
438 of the abundance and therefore prevalence of dinospores (e.g., Chambouvet *et al.*, 2008;
439 Alves-de-Souza *et al.*, 2012, 2015; Velo-Suárez *et al.*, 2013; Anderson and Harvey, 2020;
440 Sehein *et al.*, 2022). Not surprisingly, Syndiniales Group II showed seasonal patterns similar
441 to dinoflagellates, characterized by increases in abundance and richness during summer and
442 autumn, (Figs. 2, 3). The dinoflagellate abundances in this study were drastically lower than
443 most of those previously reported in coastal ecosystems. However, the abundance of
444 dinospores and the proportion of infected cells were comparable (Table 4). Given that each
445 infection produces hundreds of dinospores (Coats and Park, 2002), even a small increase in
446 the number of available hosts would result in a significant increase in the number of
447 dinospores released throughout the parasite-host dynamics (Alves-de-Souza *et al.*, 2015). The
448 strongest infection witnessed during this study (June 2018), corresponded to the highest
449 dinospore and dinoflagellate abundances (*P. minimum*) (Figs 2E and 3C), lasted more than a
450 week and reached a prevalence of 38.5% (Table 3). Prevalence in natural populations of
451 infected dinoflagellates is highly variable and can escalate up to 80% or even higher values
452 during epidemics (Coats *et al.*, 1996) though most commonly reported infection prevalence is
453 much lower (Coats and Bockstahler, 1994; Chambouvet *et al.*, 2008; Salomon *et al.*, 2009;
454 Siano *et al.*, 2011; Alves-de-Souza *et al.*, 2012; Li *et al.*, 2014, Table 4). In this study, the *P.*

455 *minimum*'s 'rise and fall' coincided with the temporal dynamics of Clade 8 and particularly to
456 a specific ASV (ASV13). Two other dinoflagellates (*Scirpsiella sp.* and *Amphidinium spp.*)
457 showed signs of infections. Although prevalence in natural dinoflagellate populations is
458 usually observed at host densities of the order of 10^5 - 10^6 L⁻¹, an infection can occur at
459 considerably lower host conditions (Salomon *et al.*, 2009). One feature that can explain our
460 observation is that dinospores are flagellated, allowing them to chase their host and thus
461 increase infection rates. Also, the ability of parasites to have a diversity of hosts could be an
462 adaptive/survival feature when certain hosts become scarce. Our study supports this
463 hypothesis since Syndiniales Group II may have had diversified larger range of hosts in
464 autumn. During the autumn peaks of dinospores, various cells presented signs of infection
465 and metabarcoding data revealed that samples were dominated by a variety of Syndiniales
466 Group II clades and ASVs. However, despite the large number of samples processed in this
467 study -at the exception of the coincidence of *P. minimum* and ASV13 in June 2018, -it
468 was not possible to evaluate the extent of specific versus non-specific infections.
469 Finally, given that the infective parasite cells have an ephemeral life (e.g., Cachon, 1964;
470 Coats and Park, 2002) and should have to rapidly find a host, one may speculate how they
471 manage to do this in such highly complex planktonic communities with low host abundances.
472 Moreover, the production of allelopathic compounds by dinoflagellates as a defense
473 mechanism killing dinospores and preventing infection (Long *et al.*, 2021) could further
474 complicate the chances of survival of these ephemeral swimmers. As such, these dinospores
475 should have their own strategies to increase the chances of finding their hosts (by chemotaxis,
476 for example); an area of research that deserves further investigation.

477

478 *Community Assembly processes of Syndiniales Group II*

479 Including parasitism in planktonic food web models is vital to better understand the

480 dynamics of hosts and parasites and to better appreciate the role of parasitism in the
481 functioning of planktonic ecosystems (e.g., Montagnes *et al.*, 2008; Salomon and Stolte,
482 2010; Alves-de-Souza *et al.*, 2015). In several studies Syndiniales dynamics have been related
483 to environmental variables such as temperature, salinity, light intensity, and nutrient
484 concentrations (Yih and Coats, 2000; Alves-de-Souza *et al.*, 2012, 2015; Li *et al.*, 2014; Käse
485 *et al.*, 2021 and references therein). In this study, a PCA (Fig. S2) revealed clear seasonal
486 patterns of environmental variables. However, multivariate analysis such as CCA and dbRDA
487 between environmental parameters and Syndiniales Group II did not show any consistent
488 pattern (data not shown). This is not surprising, since environmental variables such as the
489 ones mentioned above are not expected to have direct influence on Syndiniales Group II, but
490 affect them indirectly through the dynamics of their hosts. Here, as an alternative to
491 multivariate analysis of environmental variables and ASVs abundance, ecological processes
492 regulating the Syndiniales Group II community were explored. This exploratory analysis
493 showed the prevalence of stochastic (i.e., drift) processes in Syndiniales Group II community
494 assembly (Fig. 5B). However, June and July were the only months when part of the processes
495 could be inferred as deterministic (Fig. 5A). It is hypothesized here, that deterministic
496 processes were related to specific Syndiniales-dinoflagellate interactions observed during
497 these months (see previous section & Table 2).

498

499 In conclusion we considered both morphological and metabarcoding data using a
500 relatively large data set (287 samples) which is an approach rarely undertaken. Since
501 metabarcoding data are subjected to PCR biases and are always expressed in relative
502 abundances, and morphological data are absolute abundances but do not provide a precise
503 image of the diversity, it is important to combine these two complementary data sets. Most
504 abundant clades and ASVs affiliated to Syndiniales Group II were observed in consecutive

505 years, providing an indication of the existence of local populations, and featured consistent
506 temporal patterns. Increasing abundance and richness were always observed during the
507 second half of the year. In summer, they were related to dinoflagellate hosts; in autumn,
508 Syndiniales Group II could have more diversified hosts than earlier in the year. This is a case
509 study for coastal ecosystems presenting abundant nutrients but no dinoflagellates blooms.
510 While the dinoflagellate abundances in this study were much lower than most of those
511 previously reported in coastal ecosystems, the number of dinospores and the prevalence were
512 comparable. The low abundance of dinospores in the great majority of samples was
513 consistent with the low host abundance, indicating a stable coexistence punctuated by rare
514 transient peaks. Given all the above, the strategies of dinospores to increase their chances of
515 survival in highly complex planktonic communities and in low host abundances deserves
516 further attention. Overall, the prevalence of stochastic processes renders *a priori* less
517 predictable the seasonal dynamics of Syndiniales Group II communities to future
518 environmental change.

519

520 **Acknowledgments**

521 We would like to thank the Captain and the crew of the RV ‘Sepia II’; L. Guillou for
522 providing filters with cultures of infected dinoflagellates to test our FISH-TSA procedures, F.
523 Artigas for setting-up the DYPHYRAD sampling, M. Crouvoisier for nutrient analysis; V.
524 Cornille for help with the fieldwork, E. Goberville for meteorological data, P. Magee for
525 English proofing, the SCoSI/ULCO (Service COmmun du Système d’Information de
526 l’Université du Littoral Côte d’Opale) providing us with the computational resources to run
527 all the bioinformatic analyses via the CALCULCO computing platform ([https://www-
528 calculco.univ-littoral.fr/](https://www-calculco.univ-littoral.fr/)). This work was logistically supported by the national monitoring
529 network SOMLIT (<https://www.somlit.fr/>) and funded by the CPER MARCO

530 (<https://marco.univ-littoral.fr/>) and the French Research program of INSU-CNRS via the
531 LEFE-EC2CO 'PLANKTON PARTY' project. D.I.S was funded via a PhD grant by the
532 'Region des Hauts de France' and the 'Pôle métropolitain de la Côte d'Opale (PMCO)'.

533 **References**

- 534 Alves-de-Souza, C., Pecqueur, D., Floc'h, E.L., Mas, S., Roques, C., Mostajir, B., et al.
535 (2015) Significance of Plankton Community Structure and Nutrient Availability for
536 the Control of Dinoflagellate Blooms by Parasites: A Modeling Approach. *PLOS ONE*
537 **10**: e0127623.
- 538 Alves-de-Souza, C., Varela, D., Iriarte, J., González, H., and Guillou, L. (2012) Infection
539 dynamics of Amoebophryidae parasitoids on harmful dinoflagellates in a southern
540 Chilean fjord dominated by diatoms. *Aquat Microb Ecol* **66**: 183–197.
- 541 Aminot, A. and K erouel, R. (2004) Dissolved organic carbon, nitrogen and phosphorus in the
542 N-E Atlantic and the N-W Mediterranean with particular reference to non-refractory
543 fractions and degradation. *Deep Sea Research Part I: Oceanographic Research*
544 *Papers* **51**: 1975–1999.
- 545 Anderson, S.R. and Harvey, E.L. (2020) Temporal Variability and Ecological Interactions of
546 Parasitic Marine Syndiniales in Coastal Protist Communities. *mSphere* **5**: e00209-20.
- 547 Bower, S.M., Carnegie, R.B., Goh, B., Jones, S.R.M., Lowe, G.J., and Mak, M.W.S. (2004)
548 Preferential PCR Amplification of Parasitic Protistan Small Subunit rDNA from
549 Metazoan Tissues. *Journal of Eukaryotic Microbiology* **51**: 325–332.
- 550 Breton, E., Christaki, U., Bonato, S., Didry, M., and Artigas, L. (2017) Functional trait
551 variation and nitrogen use efficiency in temperate coastal phytoplankton. *Mar Ecol*
552 *Prog Ser* **563**: 35–49.
- 553 Breton, E., Christaki, U., Sautour, B., Demonio, O., Skouroliaou, D.-I., Beaugrand, G., et al.
554 (2021) Seasonal Variations in the Biodiversity, Ecological Strategy, and
555 Specialization of Diatoms and Copepods in a Coastal System With Phaeocystis
556 Blooms: The Key Role of Trait Trade-Offs. *Frontiers in Marine Science* **8**:
- 557 Breton, E., Rousseau, V., Parent, J.-Y., Ozer, J., and Lancelot, C. (2006) Hydroclimatic
558 modulation of diatom/Phaeocystis blooms in nutrient-enriched Belgian coastal waters
559 (North Sea). *Limnology and Oceanography* **51**: 1401–1409.
- 560 Brylinski, J.-M., Lagadeuc, Y., Gentilhomme, V., Dupont, J.-P., Lafite, R., Dupeuble, P.-A.,
561 et al. (1991) Le "fleuve cotier": Un phenomene hydrologique important en Manche
562 orientale. Exemple du Pas-de-Calais. *Oceanologica Acta* **sp**: 8.
- 563 Cachon, J. (1964) Contribution à l'étude des p ridiniens parasites. Cytologie, cycles  volutifs.
564 *Ann Sci Nat Zool* **6**: 1–158.
- 565 Callahan, B.J., McMurdie, P.J., Rosen, M.J., Han, A.W., Johnson, A.J.A., and Holmes, S.P.
566 (2016) DADA2: High-resolution sample inference from Illumina amplicon data.
567 *Nature Methods* **13**: 581–583.
- 568 Chambouvet, A., Morin, P., Marie, D., and Guillou, L. (2008) Control of Toxic Marine
569 Dinoflagellate Blooms by Serial Parasitic Killers. *Science* **322**: 1254–1257.
- 570 Chase, J.M. and Myers, J.A. (2011) Disentangling the importance of ecological niches from
571 stochastic processes across scales. *Philosophical Transactions of the Royal Society B:*
572 *Biological Sciences* **366**: 2351–2363.
- 573 Christaki, U., Courties, C., Massana, R., Catala, P., Lebaron, P., Gasol, J.M., and Zubkov,
574 M.V. (2011) Optimized routine flow cytometric enumeration of heterotrophic

575 flagellates using SYBR Green I: FC analysis of HF. *Limnol Oceanogr Methods* **9**:
576 329–339.

577 Christaki, U., Genitsaris, S., Monchy, S., Li, L.L., Rachik, S., Breton, E., and Sime-Ngando,
578 T. (2017) Parasitic Eukaryotes in a Meso-Eutrophic Coastal System with Marked
579 *Phaeocystis globosa* Blooms. *Front Mar Sci* **4**: 416.

580 Christaki, U., Kormas, K.A., Genitsaris, S., Georges, C., Sime-Ngando, T., Viscogliosi, E.,
581 and Monchy, S. (2014) Winter–Summer Succession of Unicellular Eukaryotes in a
582 Meso-eutrophic Coastal System. *Microb Ecol* **67**: 13–23.

583 Coats, D., Ej, A., Cl, G., and S, H. (1996) Parasitism of photosynthetic dinoflagellates in a
584 shallow subestuary of Chesapeake Bay, USA. *Aquatic Microbial Ecology* **11**: 1–9.

585 Coats, D.W. and Bockstahler, K.R. (1994) Occurrence of the Parasitic Dinoflagellate
586 *Amoebophrya ceratii* in Chesapeake Bay Populations of *Gymnodinium sanguineum*.
587 *Journal of Eukaryotic Microbiology* **41**: 586–593.

588 Coats, D.W. and Park, M.G. (2002) Parasitism of Photosynthetic Dinoflagellates by Three
589 Strains of *Amoebophrya* (dinophyta): Parasite Survival, Infectivity, Generation Time,
590 and Host Specificity¹. *Journal of Phycology* **38**: 520–528.

591 Doherty, S.J., Barbato, R.A., Grandy, A.S., Thomas, W.K., Monteux, S., Dorrepaal, E., et al.
592 (2020) The Transition From Stochastic to Deterministic Bacterial Community
593 Assembly During Permafrost Thaw Succession. *Frontiers in Microbiology* **11**:
594 Ellison, A.M. (1987) Effect of Seed Dimorphism on the Density-Dependent Dynamics of
595 Experimental Populations of *Atriplex Triangularis* (chenopodiaceae). *American*
596 *Journal of Botany* **74**: 1280–1288.

597 Genitsaris, S., Monchy, S., Breton, E., Lecuyer, E., and Christaki, U. (2016) Small-scale
598 variability of protistan planktonic communities relative to environmental pressures
599 and biotic interactions at two adjacent coastal stations. *Mar Ecol Prog Ser* **548**: 61–75.

600 Gleason, F.H., Kagami, M., Lefevre, E., and Sime-Ngando, T. (2008) The ecology of chytrids
601 in aquatic ecosystems: roles in food web dynamics. *Fungal Biology Reviews* **22**: 17–
602 25.

603 Grattepanche, J.-D., Breton, E., Brylinski, J.-M., Lecuyer, E., and Christaki, U. (2011)
604 Succession of primary producers and micrograzers in a coastal ecosystem dominated
605 by *Phaeocystis globosa* blooms. *Journal of Plankton Research* **33**: 37–50.

606 Grattepanche, J.-D., Vincent, D., Breton, E., and Christaki, U. (2011) Microzooplankton
607 herbivory during the diatom–*Phaeocystis* spring succession in the eastern English
608 Channel. *Journal of Experimental Marine Biology and Ecology* **404**: 87–97.

609 Guillou, L., Bachar, D., Audic, S., Bass, D., Berney, C., Bittner, L., et al. (2013) The Protist
610 Ribosomal Reference database (PR2): a catalog of unicellular eukaryote small sub-
611 unit rRNA sequences with curated taxonomy. *Nucleic Acids Res* **41**: D597-604.

612 Guillou, L., Viprey, M., Chambouvet, A., Welsh, R.M., Kirkham, A.R., Massana, R., et al.
613 (2008) Widespread occurrence and genetic diversity of marine parasitoids belonging
614 to *Syndiniales* (*Alveolata*). *Environmental Microbiology* **10**: 3349–3365.

615 Hudson, P.J., Dobson, A.P., and Lafferty, K.D. (2006) Is a healthy ecosystem one that is rich
616 in parasites? *Trends in Ecology & Evolution* **21**: 381–385.

617 Kagami, M., de Bruin, A., Ibelings, B.W., and Van Donk, E. (2007) Parasitic chytrids: their
618 effects on phytoplankton communities and food-web dynamics. *Hydrobiologia* **578**:
619 113–129.

620 Käse, L., Metfies, K., Neuhaus, S., Boersma, M., Wiltshire, K.H., and Kraberg, A.C. (2021)
621 Host-parasitoid associations in marine planktonic time series: Can metabarcoding help
622 reveal them? *PLOS ONE* **16**: e0244817.

623 Lagadeuc, Y., Bouté, M., and Dodson, J.J. (1997) Effect of vertical mixing on the vertical
624 distribution of copepods in coastal waters. *J Plankton Res* **19**: 1183–1204.

- 625 Li, C., Song, S., Liu, Y., and Chen, T. (2014) Occurrence of *Amoebophrya* spp. infection in
626 planktonic dinoflagellates in Changjiang (Yangtze River) Estuary, China. *Harmful*
627 *Algae* **37**: 117–124.
- 628 Liu, C., Cui, Y., Li, X., and Yao, M. (2021) *microeco* : an R package for data mining in
629 microbial community ecology. *FEMS Microbiology Ecology* **97**: fiae255.
- 630 Liu, C., Yao, M., Stegen, J.C., Rui, J., Li, J., and Li, X. (2017) Long-term nitrogen addition
631 affects the phylogenetic turnover of soil microbial community responding to moisture
632 pulse. *Sci Rep* **7**: 17492.
- 633 Long, M., Marie, D., Szymczak, J., Toullec, J., Bigeard, E., Sourisseau, M., et al. (2021)
634 Dinophyceae can use exudates as weapons against the parasite *Amoebophrya* sp.
635 (Syndiniales). *ISME COMMUN* **1**: 1–10.
- 636 López-García, P., Rodríguez-Valera, F., Pedrós-Alió, C., and Moreira, D. (2001) Unexpected
637 diversity of small eukaryotes in deep-sea Antarctic plankton. *Nature* **409**: 603–607.
- 638 Lorenzen, C.J. (1966) A method for the continuous measurement of in vivo chlorophyll
639 concentration. *Deep Sea Research and Oceanographic Abstracts* **13**: 223–227.
- 640 Losos, J.B. (2008) Phylogenetic niche conservatism, phylogenetic signal and the relationship
641 between phylogenetic relatedness and ecological similarity among species. *Ecology*
642 *Letters* **11**: 995–1003.
- 643 Marie, D., Brussaard, C.P.D., Thyrhaug, R., Bratbak, G., and Vaultot, D. (1999) Enumeration
644 of Marine Viruses in Culture and Natural Samples by Flow Cytometry. *Applied and*
645 *Environmental Microbiology* **65**: 45–52.
- 646 Massana, R., Gobet, A., Audic, S., Bass, D., Bittner, L., Boutte, C., et al. (2015) Marine
647 protist diversity in European coastal waters and sediments as revealed by high-
648 throughput sequencing. *Environmental Microbiology* **17**: 4035–4049.
- 649 Montagnes, D.J.S., Chambouvet, A., Guillou, L., and Fenton, A. (2008) Responsibility of
650 microzooplankton and parasite pressure for the demise of toxic dinoflagellate blooms.
651 *Aquatic Microbial Ecology* **53**: 211–225.
- 652 Morel, A. and Smith, R.C. (1974) Relation between total quanta and total energy for aquatic
653 photosynthesis. *Limnology and Oceanography* **19**: 591–600.
- 654 Park, M.G., Yih, W., and Coats, D.W. (2004) Parasites and phytoplankton, with special
655 emphasis on dinoflagellate infections. *J Eukaryot Microbiol* **51**: 145–155.
- 656 Piwosz, K., Mukherjee, I., Salcher, M.M., Grujčić, V., and Šimek, K. (2021) CARD-FISH in
657 the Sequencing Era: Opening a New Universe of Protistan Ecology. *Frontiers in*
658 *Microbiology* **12**..
- 659 R Core Team (2021) R: A language and environment for statistical computing. R Foundation
660 for Statistical Computing, Vienna, Austria.
- 661 Ramond, P., Siano, R., Schmitt, S., de Vargas, C., Marié, L., Memery, L., and Sourisseau, M.
662 (2021) Phytoplankton taxonomic and functional diversity patterns across a coastal
663 tidal front. *Sci Rep* **11**: 2682.
- 664 Rasconi, S., Jobard, M., and Sime-Ngando, T. (2011) Parasitic fungi of phytoplankton:
665 ecological roles and implications for microbial food webs. *Aquatic Microbial Ecology*
666 **62**: 123–137.
- 667 R Core Team (2021) R: A language and environment for statistical computing. R Foundation
668 for Statistical Computing, Vienna, Austria.
- 669 Redfield, A.C. (1958) The biological control of chemical factors in the environment.
670 *American Scientist* **46**: 230A–221.
- 671 Salomon, P.S., Granéli, E., Neves, M.H.C.B., and Rodriguez, E.G. (2009) Infection by
672 *Amoebophrya* spp. parasitoids of dinoflagellates in a tropical marine coastal area.
673 *Aquatic Microbial Ecology* **55**: 143–153.

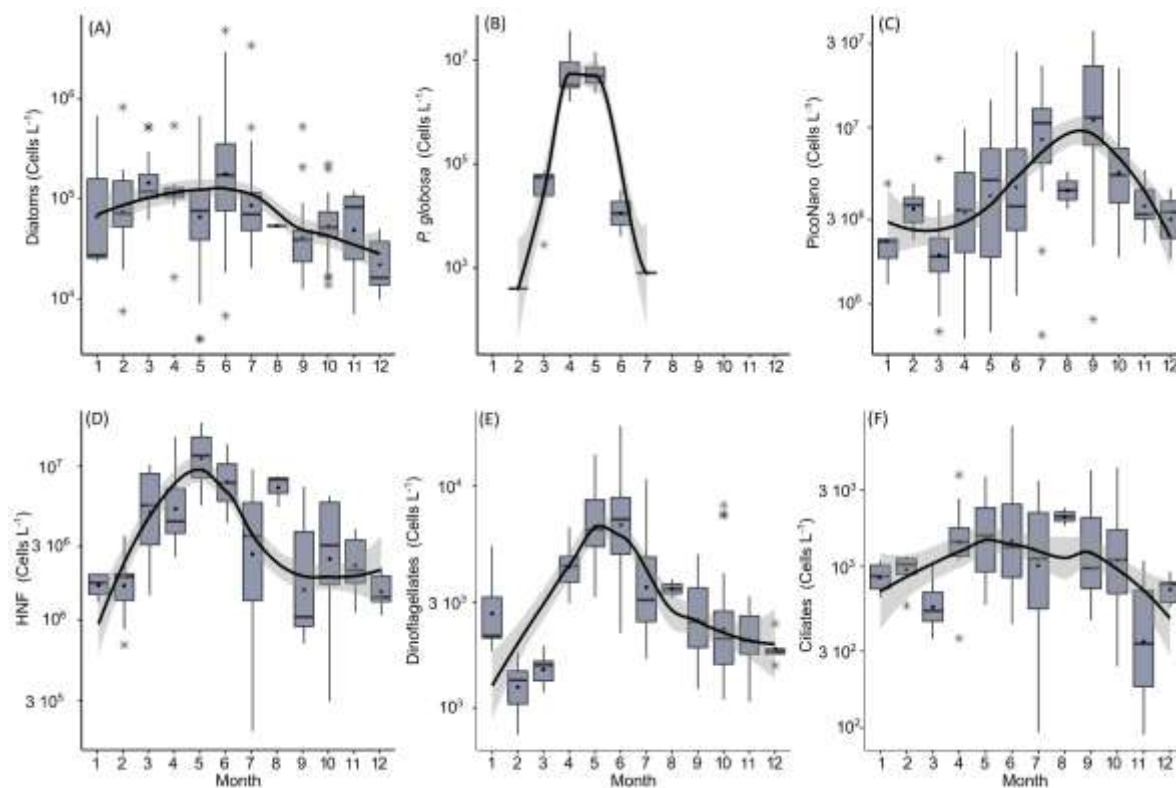
- 674 Salomon, P.S. and Stolte, W. (2010) Predicting the population dynamics in Amoebophrya
675 parasitoids and their dinoflagellate hosts using a mathematical model. *Marine Ecology*
676 *Progress Series* **419**: 1–10.
- 677 Sassenhagen, I., Irion, S., Jardillier, L., Moreira, D., and Christaki, U. (2020) Protist
678 Interactions and Community Structure During Early Autumn in the Kerguelen Region
679 (Southern Ocean). *Protist* **171**: 125709.
- 680 Sehein, T.R., Gast, R.J., Pachiadaki, M., Guillou, L., and Edgcomb, V.P. (2022) Parasitic
681 infections by Group II Syndiniales target selected dinoflagellate host populations
682 within diverse protist assemblages in a model coastal pond. *Environmental*
683 *Microbiology* **24**: 1818–1834.
- 684 Sentchev, A., Yaremchuk, M., and Lyard, F. (2006) Residual circulation in the English
685 Channel as a dynamically consistent synthesis of shore-based observations of sea level
686 and currents. *Continental Shelf Research* **26**: 1884–1904.
- 687 Shade, A., Jones, S.E., Caporaso, J.G., Handelsman, J., Knight, R., Fierer, N., and Gilbert,
688 J.A. (2014) Conditionally Rare Taxa Disproportionately Contribute to Temporal
689 Changes in Microbial Diversity. *mBio* **5**: e01371-14.
- 690 Sherr, E.B. and Sherr, B.F. (2002) Significance of predation by protists in aquatic microbial
691 food webs. *Antonie Van Leeuwenhoek* **81**: 293–308.
- 692 Siano, R., Alves-de-Souza, C., Foulon, E., Bendif, E.M., Simon, N., Guillou, L., and Not, F.
693 (2011) Distribution and host diversity of Amoebophryidae parasites across
694 oligotrophic waters of the Mediterranean Sea. *Biogeosciences* **8**: 267–278.
- 695 Skouroliakou, D.-I., Breton, E., Irion, S., Artigas, L.F., and Christaki, U. (2022) Stochastic
696 and Deterministic Processes Regulate Phytoplankton Assemblages in a Temperate
697 Coastal Ecosystem. *Microbiology Spectrum* **0**: e02427-22.
- 698 Skovgaard, A. (2014) Dirty Tricks in the Plankton: Diversity and Role of Marine Parasitic
699 Protists. *Acta Protozoologica* **53**:
- 700 Smayda, T.J. (2002) Turbulence, watermass stratification and harmful algal blooms: an
701 alternative view and frontal zones as “pelagic seed banks.” *Harmful Algae* **1**: 95–112.
- 702 Smith, S.D. (1988) Coefficients for sea surface wind stress, heat flux, and wind profiles as a
703 function of wind speed and temperature. *Journal of Geophysical Research: Oceans*
704 **93**: 15467–15472.
- 705 Stegen, J.C., Lin, X., Fredrickson, J.K., Chen, X., Kennedy, D.W., Murray, C.J., et al. (2013)
706 Quantifying community assembly processes and identifying features that impose
707 them. *ISME J* **7**: 2069–2079.
- 708 Stegen, J.C., Lin, X., Konopka, A.E., and Fredrickson, J. (2012) Stochastic and deterministic
709 assembly processes in subsurface microbial communities. *The ISME Journal* **12**.
- 710 Velo-Suárez, L., Brosnahan, M.L., Anderson, D.M., and McGillicuddy Jr, D.J. (2013) A
711 quantitative assessment of the role of the parasite Amoebophrya in the termination of
712 Alexandrium fundyense blooms within a small coastal embayment. *PLoS One* **8**:
713 e81150.
- 714 Xu, Z., Cheung, S., Endo, H., Xia, X., Wu, W., Chen, B., et al. (2022) Disentangling the
715 Ecological Processes Shaping the Latitudinal Pattern of Phytoplankton Communities
716 in the Pacific Ocean. *mSystems* **7**: e01203-21.
- 717 Yih, W. and Coats, D.W. (2000) Infection of *Gymnodinium sanguineum* by the
718 Dinoflagellate Amoebophryasp.: Effect of Nutrient Environment on Parasite
719 Generation Time, Reproduction, and Infectivity. *J Eukaryotic Microbiology* **47**: 504–
720 510.
- 721 Zhou, J. and Ning, D. (2017) Stochastic Community Assembly: Does It Matter in Microbial
722 Ecology? *Microbiol Mol Biol Rev* **81**:

723

724

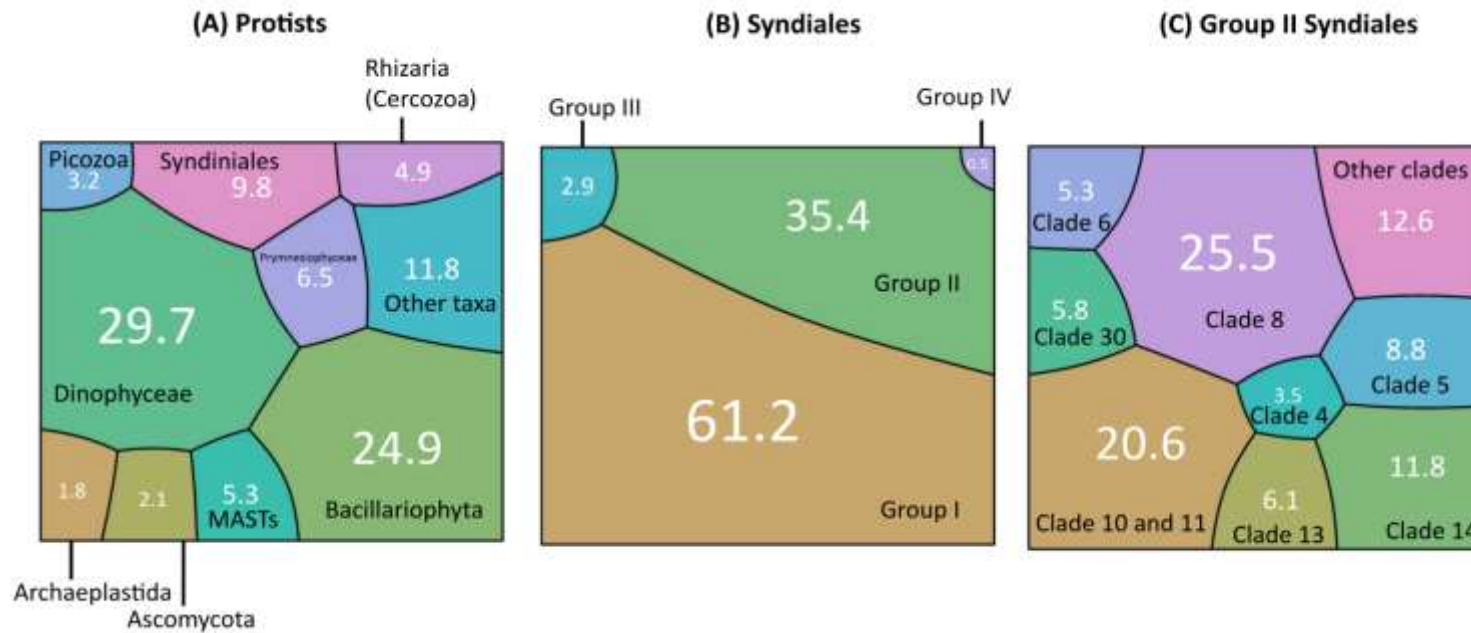
725

726



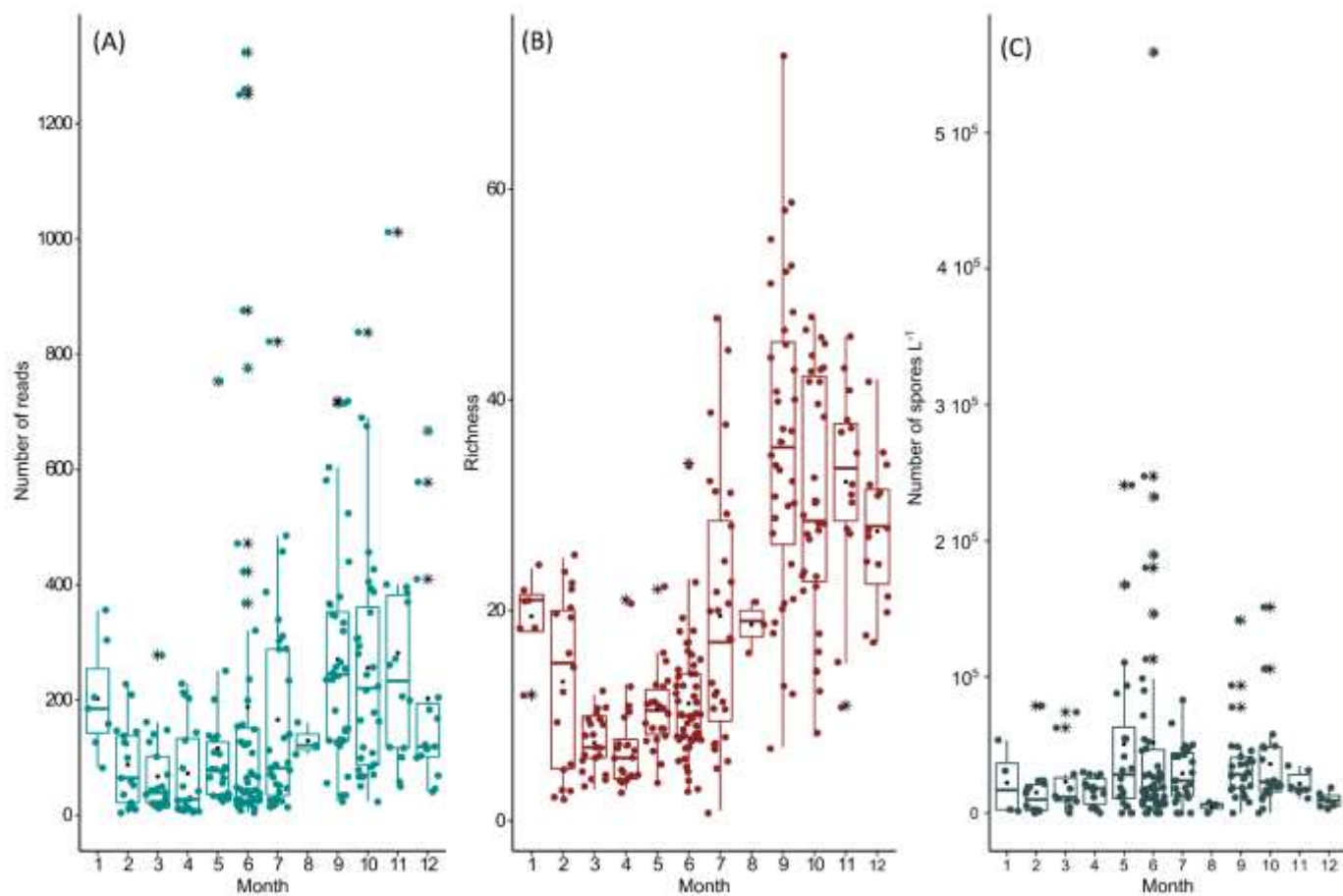
728

729 **Figure 1.** Seasonal variation of protist abundance (cells L⁻¹): (A) Diatoms, (B) *P. globosa*, (C) PicoNano: pico- nanophytoplankton, (D) HNF: heterotrophic
 730 nanoflagellates, (E) dinoflagellates, and (F) ciliates, identified in the eastern English Channel at the SOMLIT and DYPHYRAD stations from March 2016 to
 731 October 2020. Y scale is log₁₀ transformed. Solid black lines in the boxplot represent the median, black dots the mean, and the black stars the outliers. The
 732 solid line and ribbon represent LOESS smoothing and the 95% confidence interval. Data for ciliates and dinoflagellates were available for 2018-2020



733

734 **Figure 1.** Voronoi diagrams representing the relative abundance, given in percentage, of different protist taxonomies from 2016 to 2020 in the eastern English
 735 Channel at the SOMLIT (S1, S2) and DYPHYRAD (R1, R2, and R4) stations. The area of each cell being proportional to the taxa relative abundance (the
 736 specific shape of each polygon carries no meaning). This type of visualization is similar to pie charts but represents better small contributors (A) Relative
 737 abundance of the nine identified supergroups, (B) Relative abundance of Dino-Group Syndiniales within the taxonomic Class Syndiniales, (C) Relative
 738 abundance of Clades within Group II Syndiniales. Visualisation performed using the online tool <http://www.bioinformatics.com.cn/srplot>.

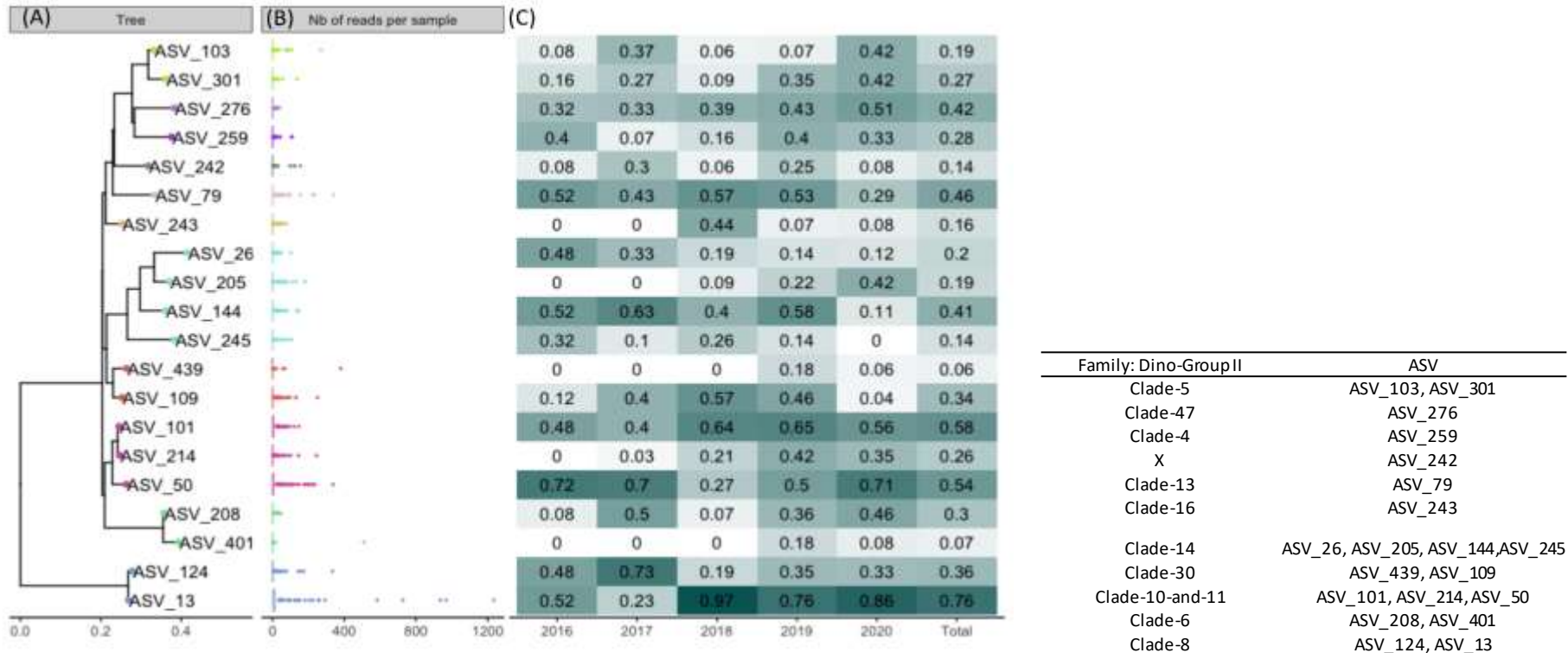


739

740 **Figure 3.** Seasonal variation of Group II Syndiniales in the eastern English Channel at the SOMLIT and DYPHYRAD stations. **(A)** Number of reads, **(B)**

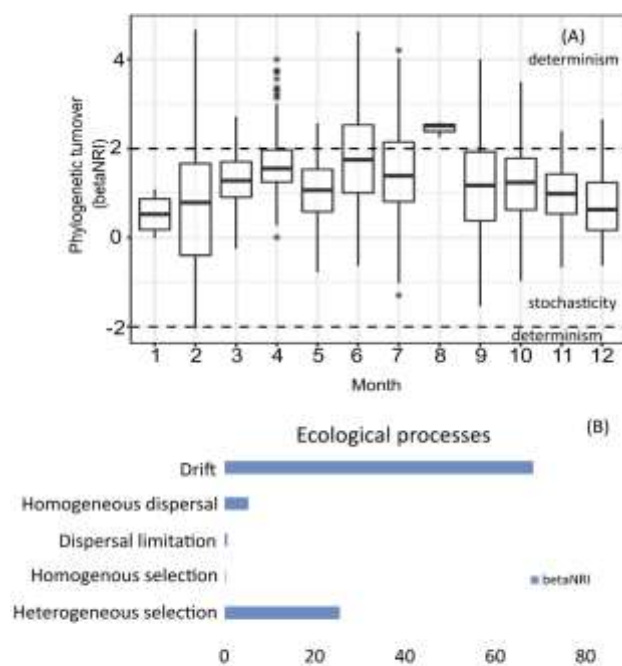
741 Richness, **(C)** Dinospores. Solid lines in the boxplot represent the median, black dots the mean, and the black stars the outliers.

742



743

744 **Figure 4.** Maximum likelihood tree of the 20 most abundant Group II Syndiniales ASVs (ASVs representing at least 1% of the Syndiniales affiliated reads on
745 the rarefied dataset); **(B)** Boxplots of the number of reads per sample. Note that for all boxplots the median value is close to zero and high abundances are
746 visible as outliers **(C)** ASV's relative abundance in samples where at least one read of each ASV was present for each year (2016-2020). **The**
747 **intensity of the color corresponds to the relative abundance.** To note that the number of samples differs between the years as follows 2016 : 26
748 samples, 2017 : 30 samples, 2018 : 76 samples, 2019 : 72 samples and 2020 : 65 samples.



750

751 **Figure 5. (A)** Phylogenetic turnover index (β NRI) Group II Syndiniales ASVs in the eastern English Channel at the SOMLIT and DYPHYRAD stations from
 752 March 2016 to October 2020. Solid black lines represent the median and black dots the mean. β NRI > 2, β NRI < -2 indicating deterministic processes and
 753 $-2 < \beta$ NRI < 2 indicattin stochastic processes (see also Table 2). **(B)** Relative importance of the ecological processes driving Group II Syndiniales communities in
 754 the eastern English Channel at the DYPHYRAD and SOMLIT stations from March 2016 to October 2020. *Note that only three samples were available for*
 755 *August – data not interpretable.*

756 **Tables**

757 Table 1. Station and sample description. Max. depth corresponds at highest tide. To note that S1 and R1 being closer to the coast were easier to sample under
 758 difficult weather conditions (see also Fig. S1). Environmental parameters and 18S rDNA amplicon sequencing were realized for all 2016-2020 samples.
 759 Microscopy counts of microplankton, flow cytometry and FISH-TSA for 2018-2020 samples at all stations (total 269 samples).

760

Sta.	Date	Long (°E)	Lat (°N)	Max. depth	Distance from the coast (km)	Sampling Frequency	No of samples
S1	2016-2020	1.3117	50.4075	27	2	Bi-weekly	63
S2	2016-2020	1.2460	50.4075	56	9.8	Bi-weekly	39
R1	2018-2020	1.3360	50.4760	19	2.6	Once/twice a week	79
R2	2018-2020	1.3231	50.4760	23	4.3	Once a week	42
R4	2018-2020	1.2780	50.4760	52	10.9	Once/twice a week	46

761

762

763 Table 2. Prevalence (%) of infected hosts identified in [individual](#) samples where it was possible to count at least 50 morphologically recognizable
 764 potential hosts were observed (for station position see Table 1 and Fig. S1). [The clades present at each date are detailed in Fig.S5](#)
 765

Station,	R1	R1	R2	R1	S1	R1	R1	R1
Date	05/06/2018	06/06/2018	07/06/2018	08/06/2018	12/06/2018	14/11/2018	05/07/2019	09/10/2019
Prevalence (%)	11.5	10.5	4.7	38.5	17.6	9.1	12.8	14.3
Infected protist	<i>P. minimum</i>	<i>P. minimum</i>	<i>P. minimum</i>	<i>P. minimum</i>	<i>P. minimum</i> <i>Amphidinium</i> sp	various	<i>Scropsiella</i> sp. <i>P. minimum</i>	various

766

767

768 Table 3. Definitions of the different assembly processes, and respective model conditions referenced from Webb 2002, Stegen et al. (2012, 2013) and Zhou
 769 and Ning (2017).

	Deterministic processes		Stochastic processes		
	Homogeneous selection	Heterogeneous selection	Dispersal limitation	Homogeneous dispersal	Drift
<i>Definition</i>	Consistent biotic (i.e., hosts) or abiotic factors cause low compositional turnover	Shifts in biotic (i.e., hosts) or abiotic factors cause high compositional turnover	Movement of individual is restricted	High rate of movement of an individual from one location to another	Population size fluctuates due to chance events
<i>Phylogenetic turnover index</i>	$\beta\text{NRI} < -2$	$\beta\text{NRI} > 2$		$-2 < \beta\text{NRI} < 2$	
<i>Taxonomic turnover index</i>	-	-	$\text{RC}_{\text{bray}} > 0.95$	$\text{RC}_{\text{bray}} < -0.95$	$-0.95 < \text{RC}_{\text{bray}} < 0.95$

770

771

772

773 Table 4. Comparative table between the present and several previous studies Widdicombe *et al.* 2010 and Grattepanche *et al.* 2011 studies are reported for
774 comparison with the dinoflagellate abundances of the present study.

775

Dinoflagellates 10^3 L^{-1}	Dinospores 10^3 L^{-1}	Prevalence (% of infected protists)	site	observations	references
Max ~400	Max ~800	Mean 21 Max 46	Penzé estuary (northern Brittany, France)	June, during dinoflagellate bloom	Chambouvet <i>et al.</i> 2008
Mean 70 Min <1 Max >500 <i>Prorocentrum</i> up to 3360	ND	ND	Western English Channel (coastal)	Year round , Weekly, 15 years	Widdicombe <i>et al.</i> 2010
Mean 5.3 Min 0.3 Max 32.4	ND	ND	Eastern English Channel (station S1, Fig. S1)	Year round , Bi-weekly 52 samples	Grattepanche <i>et al.</i> 2011
ND	Min 4.2 Max 1500	Min ~1 Max 25	Mediterranean	Summer, East-West transect	Siano <i>et al.</i> 2011
Min < 10 Max >100 <i>Prorocentrum</i> up to 103	Max 1680	Min undetectable Max ~12	Reloncaví Fjord, southern Chile (coastal)	Summer, bi-weekly during <i>Prorocentrum</i> bloom	Alves-de-Souza <i>et al.</i> 2012
Range ~ 1-1000	Min < 0.1 Max 1000	Min undetectable Max ~70	Salt pond (Eastham, MA USA)	March-May, 1-3 days, 13 samples	Velo-Sarez <i>et al.</i> 2013
ND	Min 0 Max 335	Min 0 Max 2.56	Salt pond (Falmouth, MA, USA)	March-October, twice a week	Sehein <i>et al.</i> 2022
Mean 4.5 Min 0.76 Max 18.6 <i>Prorocentrum</i> up to 15	Mean 35.5 Min 0 Max 559	Min undetectable Max 38.5	Eastern English Channel (coastal, Fig. S1)	Year round, One/ twice a week, 205samples	This study

776